Research Article

Zhili Li, Zhihao Xie, Dongsheng He*, Jie Deng, Hengqin Zhao, and Hongqiang Li

Simultaneous leaching of rare earth elements and phosphorus from a Chinese phosphate ore using H_3PO_4

https://doi.org/10.1515/gps-2021-0023
received December 30, 2020; accepted March 02, 2021

Abstract: Although phosphate rock has been considered as a potential new rare earth elements (REEs) resource, the recovery of REEs from phosphate rock is impeded by technical challenges and cost issues. This study investigated the effects of operation conditions on the leaching efficiencies of REEs and phosphorus from Zhijin phosphate ore, a large phosphate deposit in China. The leaching process overtime was also studied by chemical analysis, scanning electron microscope with energy dispersive spectroscopy (SEM-EDS), and X-ray diffraction (XRD). The results indicated that the REEs from Zhijin phosphate ore were mainly present in fluorapatite and dolomite, and REEs had similar trends of leaching efficiency to those of phosphorus and magnesium. Under the conditions of 25 wt% phosphoric acid concentration in the initial pulp, a weight ratio of liquid to solid of 12 mL/g, a temperature of 60°C, an agitation speed of 220 rpm, and leaching time of 120 min, REEs and phosphorus leaching efficiencies of 97.8% and 99.7% were obtained. Most parts of dissoluble substances were decomposed within 30 min. Chemical analysis, SEM-EDS, and XRD results indicated that leaching efficiencies of minerals in Zhijin phosphate ore increased following the order: quartz, aluminosilicate, pyrite, fluorapatite, dolomite, and calcite.

Keywords: rare earth elements, phosphate ore, acid leaching, phosphoric acid

1 Introduction

Rare earth elements (REEs) have been considered as the critical materials in the world due to their specialized application in many modern technologies [1,2]. Due to a global supply shortage and strengthening demand of REEs, the exploration and processing of new sources (known as secondary sources) of REEs are necessary [3]. Phosphate rock is the most significant secondary REEs resource [4], and it contains 0.046 wt% REEs on average [5]. About 50 million tons of rare earths are stored in phosphate resources worldwide, nearly one hundred thousand of which are mined annually in the production of phosphate rock [6]. In phosphate rock, REEs occur primarily in the form of isomorphous substitution for Ca and deposit as the REE-francolite that can be easily released into leaching solution by mineral acids [7]. A small amount of REEs are present as particle inclusions such as monazite, xenotime, allanite, and carbonate in apatite, which result in difficulty in REEs dissolution during the leaching process [5].

Researchers have investigated the dissolving of REEs and phosphorus by HNO_3 [8,9], HCl [5,10,11], H_2SO_4 [6,12,13], H_3PO_4 [14–16], and organic acids [17,18]. However, at present, phosphate rock is principally enriched by flotation process first, and then, the flotation concentrate is decomposed by H_2SO_4 process, producing phosphoric acid and phosphogypsum (an industrial waste produced by wet-process phosphoric acid). During the flotation process, 40% of the REEs enter the waste clay

* **Corresponding author: Dongsheng He,** Xingfa School of Mining Engineering, Wuhan Institute of Technology, Wuhan 430073, Hubei, China, e-mail: csuhy@126.com
Zhili Li: Xingfa School of Mining Engineering, Wuhan Institute of Technology, Wuhan 430073, Hubei, China; State Environmental Protection Key Laboratory of Mineral Metallurgical Resources Utilization and Pollution Control, Wuhan University of Science and Technology, Wuhan 430081, Hubei, China
Zhihao Xie: Xingfa School of Mining Engineering, Wuhan Institute of Technology, Wuhan 430073, Hubei, China; Kunming Metallurgical Research Institute, Kunming 650031, Yunnan, China
Jie Deng: Institute of Multipurpose Utilization of Mineral Resources, Chinese Academy of Geological Sciences, Chengdu 610041, Sichuan, China
Hengqin Zhao: Institute of Multipurpose Utilization of Mineral Resources, Chinese Academy of Geological Sciences, Zhengzhou 450006, Henan, China
Hongqiang Li: Xingfa School of Mining Engineering, Wuhan Institute of Technology, Wuhan 430073, Hubei, China

(phosphatic clay or slimes), 10% into sand tailings, and the remaining 50% into phosphate concentrate [6]. In addition, a substantial amount of phosphorous is lost in the flotation tailings. In the wet-process, 37.5% of the total REEs end up in phosphogypsum, and 12.5% enter phosphoric acid and fertilizer [6]. As a result, extra processes are required to recover REEs from these products. In the H_3PO_4 process, phosphate ore containing REEs and phosphorous is decomposed by H_3PO_4, forming $Ca(H_2PO_4)_2$, $REE(H_2PO_4)_3$, and insoluble substance [15]. After filtering, REEs are recovered by precipitation, crystallization, solvent extraction, and ion exchange [19–21]. $H_2PO_4^-$ is recovered by H_2SO_4, producing phosphoric acid and high-quality gypsum. Among these acid leaching processes, H_3PO_4 process is considered as one of potential promising processes for REEs' recovery since it does not introduce extra ion impurities in the leaching system and enrich REEs in leaching solution [3]. With regard to leaching of REEs and phosphorous from phosphate, Wu et al. investigated the effect of L/S ratio, concentration of phosphoric acid, temperature, and leaching time on the leaching efficiency of REEs and other major components using Fanshan phosphate of P_2O_5, MgO, and SiO_2 content of 33.65%, 1.39%, and 3.71%, respectively [3]. Simultaneous leaching of REEs and phosphorus from crude phosphate ore without flotation previously with phosphoric acid can avoid the loss of REEs and phosphorus during the flotation process, and the loss of REEs in gypsum. However, further investigation for the leaching of REEs and phosphorus simultaneously through this process is needed for lack of systematical study.

In this paper, Zhijin phosphorite deposit in China was used to investigate the influence of operation conditions on leaching process, and the leaching residue over time was characterized to study the variation of different minerals in leaching process.

2 Materials and methods

2.1 Materials

The phosphate ore containing REEs was obtained from Guizhou Zhijin in China. It was crushed and wet ground to get samples for acid leaching and scanning electron microscope with energy dispersive spectroscopy (SEM-EDS) tests, and further grinding was conducted to obtain samples for chemical analysis and inductively coupled plasma-optical emission spectrometry (ICP-OES) test. Chemical analysis (XRF) of the phosphate ore is shown in Table 1 and the partitioning of rare earth oxides conducted by ICP-OES test is displayed in Table 2. According to the data in Tables 1 and 2, this phosphate ore was a low-grade calcium siliceous phosphate with P_2O_5 content of 17.12%. The REEs content was 0.10 wt%, about two times of the average REEs content in general phosphate ores [5]. The proportion of light REEs was slightly higher than that of heavy REEs. La, Ce, Nd, and Y were the main REEs in the sample. The mineral composition of Zhijin phosphate ore was analyzed by Mineral Liberation Analyser and the results are shown in Table 3. Fluorapatite was the main phosphate mineral, and the content was 40.86%. Dolomite, quartz, aluminosilicate, calcite, and pyrite were the main gangue minerals. No independent rare earth minerals were found in this phosphate ore. The distribution of REEs was detected by SEM-EDS, and the main results are present in Figures 1 and 2. It shows that REEs were mainly found in fluorapatite and dolomite. Content of La, Ce, Nd, and Y in fluorapatite were 0%, 0.01%, 0%, and 0.04%, respectively, and the content of these elements in dolomite were 0.01%, 0.04%, 0.01%, and 0%, respectively. Analytical grade phosphoric acid (>85% H_3PO_4) produced by Tianjing Chemical Works was used. All other chemicals used were of analytical reagent grade. Distilled water was used in all the experiments.

2.2 Leaching tests

For the acid leaching experiments, the acid solution with the desired concentration was prepared in a 250 mL flask and heated on a temperature-controlled water bath equipped with a magnetic stirrer that was able to maintain the temperature with an accuracy of ± 1°C. Then, a desired amount of phosphate ore (−0.074 mm = 83.8%) was added to the acid solution. A predetermined stirring speed was maintained for Teflon-coated stirring bar. After leaching for a desired time, the suspensions were

Table 1: Chemical analysis of Zhijin phosphate ore (wt%)

Oxides	P_2O_5	CaO	MgO	SiO_2	Fe_2O_3	Al_2O_3	F	S	ΣREO	Others	LOI
Content	17.12	39.83	7.77	14.77	1.97	1.84	1.88	0.93	0.10	0.56	13.23

Table 2: Partitioning of REO in Zhijin phosphate ore ($\times 10^{-6}$)

Oxides	La_2O_3	CeO_2	Pr_6O_{11}	Nd_2O_3	Sm_2O_3	Eu_2O_3	Gd_2O_3
Content	196.84	139.63	33.15	139.45	25.79	6.61	31.82
Oxides	**Tb_4O_7**	**Dy_2O_3**	**Ho_2O_3**	**Er_2O_3**	**Tm_2O_3**	**Yb_2O_3**	**Lu_2O_3**
Content	4.67	26.74	5.98	15.87	2.80	9.37	1.91
Oxides	**Y_2O_3**	**Sc_2O_3**	**ΣREO**	**ΣLREO**	**ΣHREO**	**δCe**	**δEu**
Content	366.90	9.78	1017.31	541.47	475.84	0.36	1.00

Table 3: Mineral composition and content in Zhijin phosphate ore (wt%)

Composition	Dolomite	Fluorapatite	Quartz	Wollastonite	Calcite	Pyrite
Content	33.65	40.86	12.11	6.17	3.11	1.23
Composition	**Muscovite**	**Anorthite**	**Limonite**	**Others**	**Total**	
Content	0.93	0.84	0.15	0.95	100	

filtered, dried, and weighed to get the samples for analyses. For each condition, at least three repeated tests were performed, and the average leaching efficiencies were reported in this work.

2.3 Chemical analysis

The concentration of various ions in the aqueous solutions was measured by an inductively coupled plasma-optical emission spectrometer (ICPS-7000 ver. 2 Shimadzu, Japan). Several solid samples were determined by ICP-OES after acid dissolution (combination of perchloric acid, hydrofluoric acid, and nitric acid). The analytical precision for ICP-OES in terms of the relative standard deviation of replicate analyses was less than 5%.

2.4 SEM-EDS measurements

Quanta 250 SEM (FEI, USA) was used to determine the attribution of REEs in Zhijin phosphate ore as well as the

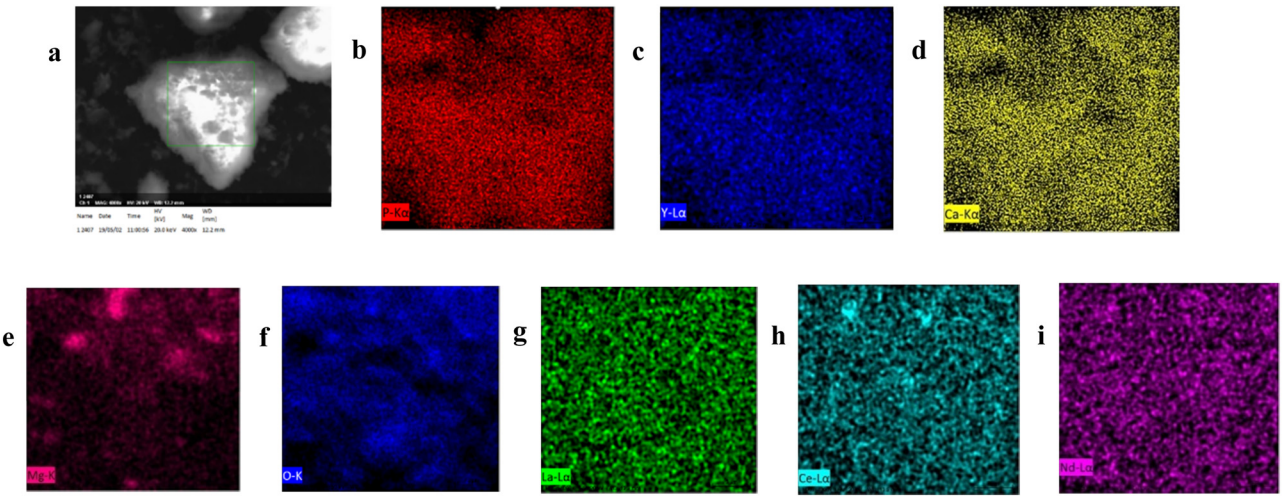

Figure 1: SEM-EDS image of a fluorapatite particle from which EDS elemental maps were obtained; (a) was a SEM image for fluorapatite particle; (b–i) were elemental maps for P, Y, Ca, Mg, O, La, Ce, and Nd, respectively.

nature, morphology, and particle size variation before and after leaching. Before the SEM-EDS tests, the samples were sputter-coated with a layer of gold.

2.5 X-ray diffraction (XRD) analysis

The sample phase and crystallinity were analyzed using a Bruker D8 Advanced X-ray diffractometer with a one-dimensional detector and a Cu Kα irradiation source (λ = 1.5406 Å) at 40 kV, 40 mA, and room temperature. The Zhijin phosphate ore leached for different time was rinsed, dried, and ground for XRD measurement. The samples were scanned in reflection mode in the 2θ range from 10° to 80° with a step size of 0.02° and a collection time of 2.5 s/step.

3 Results and discussion

3.1 Effect of initial phosphoric acid concentration in pulp

Since H^+ concentration in the pulp is closely related to mineral digestion speed, it exerts a critical influence on REEs and P_2O_5 leaching efficiencies [12]. Figure 3 shows the leaching efficiency of phosphate and REEs as a function of phosphoric acid concentration in initial leaching pulp. Since La, Ce, Nd, and Y were the main REEs in the phosphate sample, their leaching efficiencies were also plotted. The leaching efficiencies of REEs and P_2O_5 increased sharply with increasing concentration of phosphoric acid, reaching a plateau at concentration of 25% with more than 96% and 97% leaching efficiency of REEs and P_2O_5, respectively. With further increase of phosphoric acid concentration, the leaching efficiencies of REEs and P_2O_5 were kept virtually constant. In the phosphoric acid concentration range studied, the increased trends of REEs and P_2O_5 leaching efficiency were almost the same, which is consistent with the fact that in phosphate ore, REEs present majorly in the form of isomorphous substitution for Ca and deposit as the REE phosphate [22]. Below phosphoric acid concentration of 25%, the H^+ available for phosphate digestion increased with the increase of phosphoric acid concentration, leading to a dramatic rise in leaching efficiency [15]. However, above phosphoric acid concentration of 25%, the H^+ for phosphate digestion was saturated and excessive H^+ was not able to participate in the reaction, so further increase of phosphoric acid concentration has little effect on the leaching efficiencies. Hence, phosphoric acid concentration of 25% was used in the following experiments.

3.2 Effect of ratio of liquid to solid

The effect of liquid to solid ratio on REEs and P_2O_5 leaching efficiency was tested in the range of 3 to 15 mL/g, and the results are shown in Figure 4. The REEs and P_2O_5 leaching efficiency increased drastically first as the ratio rose until it reached a platform, about 96% and 97% leaching efficiencies of REEs and P_2O_5, respectively, at

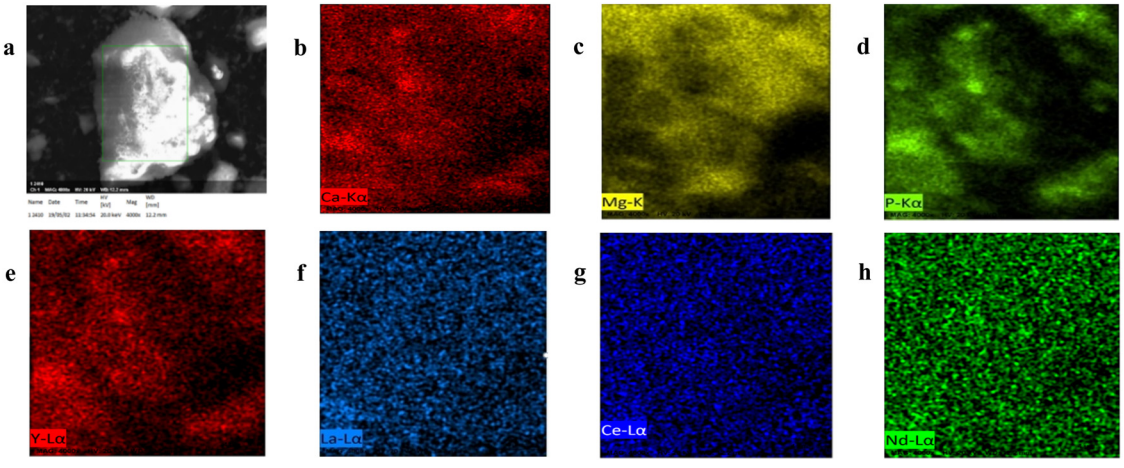

Figure 2: SEM-EDS image of a dolomite particle from which EDS elemental maps were obtained; (a) was a SEM image for dolomite particle; (b–h) were elemental maps for Ca, Mg, P, Y, La, Ce, and Nd, respectively.

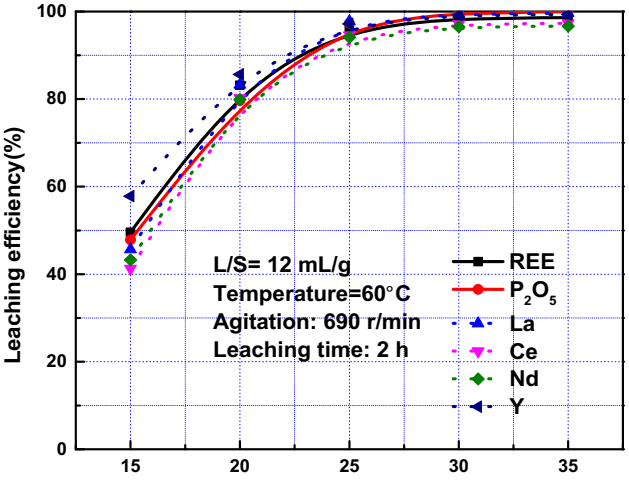

Figure 3: Leaching efficiencies of REE and P_2O_5 as a function of phosphoric acid concentration in initial leaching pulp.

the ratio of liquid to solid of 12 mL/g. Further increase of liquid to solid ratio had little effect on the leaching efficiency. As the liquid to solid ratio increased, the viscosity of the leaching pulp decreased, and thus, the diffusion speed of ions on phosphate surface increased, resulting in accelerated acidolysis rate [12]. In addition, the concentration of various insoluble substances produced was reduced with the increase of liquid to solid ratio, making it difficult to adhere to the surface of minerals, and thus, reducing its negative influence on the decomposition of minerals. In order to get higher leaching efficiencies, liquid to solid ratio of 12 mL/g was utilized in the following experiments.

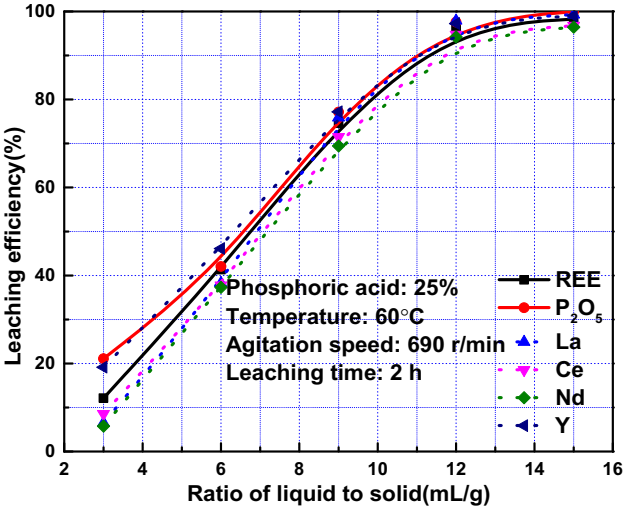

Figure 4: Leaching efficiencies as a function of ratio of liquid to solid.

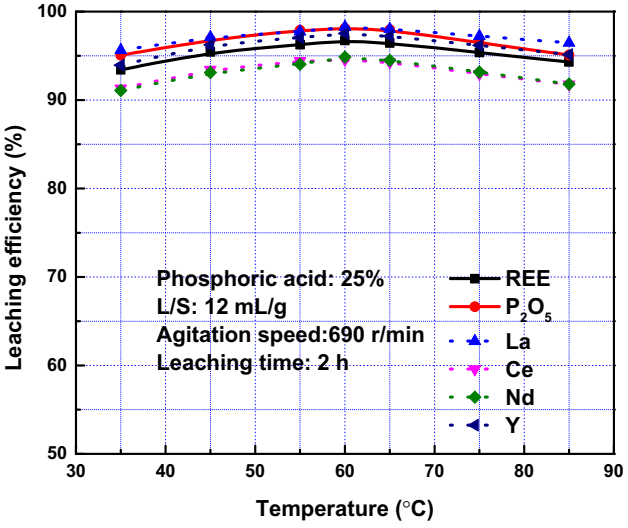

Figure 5: Leaching efficiencies as a function of leaching temperature.

3.3 Effect of temperature

Figure 5 presents the leaching efficiencies of REEs and P_2O_5 as a function of temperature. The leaching efficiencies increased with the increase of temperature, reached the maximum at 60°C, and dropped with further increase of leaching temperature. Increasing temperature will lead to two competing effects on the leaching efficiency. Equations 1–3 were endothermic and occurred simultaneously in the whole temperature range studied. Equations 1 and 2 describe the dissolution of REEs and phosphorous in phosphoric acid solutions, whereas Eq. 3 is the process forming the $REEPO_4$ precipitates. At temperature below 60°C, the viscosity of the pulp reduced with the increase of temperature, which is beneficial to the diffusion of H^+, leading to the increase of leaching efficiency. In addition, the reaction of H^+ with fluorapatite and dolomite (Eq. 1 and 2) is endothermic and plays a major role. Thus, increasing the temperature accelerated the attacking of H^+ on fluorapatite and dolomite at temperature below 60°C, and therefore, the leaching efficiencies of REEs and phosphorous increased. However, the solubility of REEs in mixture solution of $Ca(H_2PO_4)_2$–H_3PO_4 decreased with temperature increasing and insoluble REE phosphate was formed, especially at high temperature [5,6]. Formation of $REEPO_4$ precipitates (Eq. 3) played an increasingly important role with the increase of temperature. Therefore, the leaching efficiencies of REEs and phosphorous reduced at temperature above 60°C. Thus, 60°C was set in the following leaching tests.

$$Ca_{5-2x}(REE,Na/K)_xF(PO_4)_3 + 7H_3PO_4 = (5-2x)Ca(H_2PO_4)_2 + xREE(H_2PO_4)_3 + x(Na/K)H_2PO_4 + HF \quad (1)$$

$$MgCa(REE,Na/K)_x(CO_3)_{2+2x} + (4x+4)H_3PO_4 = Mg(H_2PO_4)_2 + Ca(H_2PO_4)_2 + xREE(H_2PO_4)_3 + x\left(\frac{Na}{K}\right)H_2PO_4 + (2+2x)H_2O + (2+2x)CO_2\uparrow \quad (2)$$

$$REE^{3+} + H_nPO_4^{n-3} = REEPO_4\downarrow + nH^+ \quad (3)$$

3.4 Effect of agitation speed

Another parameter on which the extent of dissolution of phosphate ore in acidic media depends is the speed of agitation. During these experiments, the temperature was kept at 60°C, and H_3PO_4 of 25% was used. As shown in Figure 6, the leaching efficiencies increased significantly with the increase of stirring speed, reaching a plateau at 220 rpm. At speed above 220 rpm, this effect became less remarkable. At speed below 220 rpm, the increase of the agitation enhanced the diffusion of H^+ to the surface of phosphate and dolomite [14], and the leached ions were able to transfer rapidly from the surface of phosphate and dolomite to acid solution; as a result, the leaching efficiencies were promoted. Therefore, agitation speed of 220 rpm was performed in the following leaching tests.

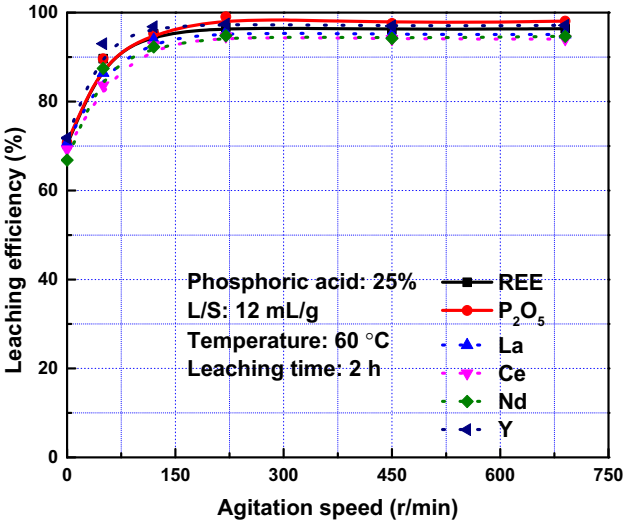

Figure 6: Leaching efficiencies as a function of agitation speed.

3.5 Effect of leaching time

Leaching time is an important kinetic parameter for leaching processes of minerals since it is the judgment basis of reaction equilibrium. Therefore, the effect of leaching time on leaching efficiencies of REEs and P_2O_5 was investigated in 25% phosphoric acid with stirring speed 220 rpm, L/S = 12:1 mL/g at 60°C. As shown in Figure 7, the most part of dissoluble REEs and P_2O_5 were decomposed in the first half an hour. The increasing trend of leaching efficiencies became mild after leaching for 30 min. This demonstrates that further prolonging leaching time would not bring significant improvement of leaching efficiency. From the point of view of shortening leaching time and optimizing leaching efficiency, 120 min was considered as the proper leaching time. Thus, the optimum leaching conditions for Zhijin phosphate ore using phosphoric acid were listed as follows: phosphoric acid concentration in the initial leaching pulp of 25–35%, temperature of 60°C, ratio of liquid to solid of 12–14 mL/g, agitation speed of 220 rpm, and leaching time of more than 120 min. With phosphoric acid concentration of 25%, temperature of 60°C, ratio of liquid to solid of 12 mL/g, agitation speed of 220 rpm, and leaching time of 120 min, chemical composition of the leachate is (g/L): REO = 0.086, CaO = 32.32, MgO = 6.41, Fe_2O_3 = 0.79, Al_2O_3 = 0.40, F = 1.43, S = 0.29. Solvent extraction, ion exchange, and precipitation have been used to recover REEs from pregnant leaching solutions obtained from acid leaching [23]. In the 1960s, ion exchange was the only practical method to recover REEs from leachate [23]. Nowadays, solvent extraction is the most widely used approach [23]. However, large amount of waste is generated during the processes and toxic chemicals are

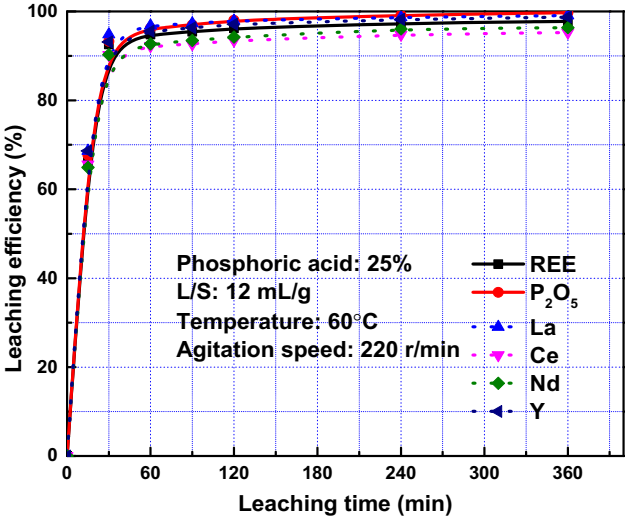

Figure 7: Leaching efficiencies as a function of leaching time.

Table 4: Chemical analysis of leaching residue after different leaching time (wt%)

Leaching time (min)	P_2O_5	SiO_2	CaO	MgO	Fe_2O_3	Al_2O_3	F	SO_3
0	17.12	14.77	39.83	7.77	1.97	1.84	1.88	0.93
30	8.16	61.59	11.06	1.18	5.18	6.52	0.931	2.41
60	5.77	66.33	7.56	1.19	5.57	7.03	0.917	2.63
120	2.86	72.15	3.93	1.21	6.05	7.12	0.799	2.89
240	1.37	75.10	2.04	1.23	6.15	7.21	0.939	2.90

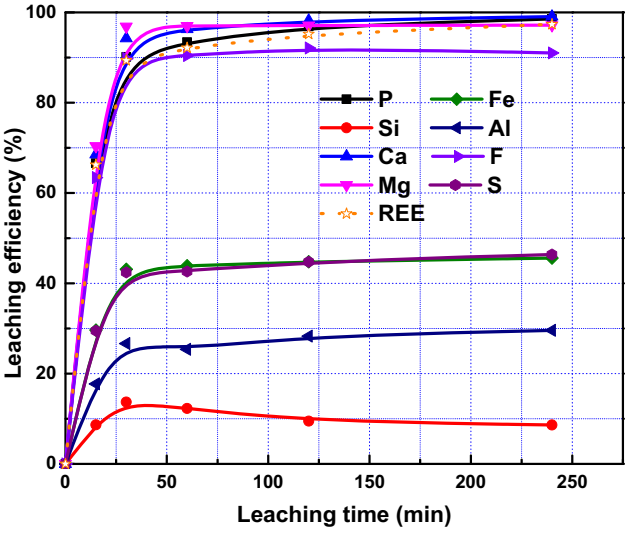

Figure 8: Leaching efficiencies of various elements as a function of leaching time.

often used [24]. It has been reported that solubility of REEs at 90°C in phosphate acid solution is very low [3]. The most promising method to recover REEs and phosphorous simultaneously is to form precipitate of rare earth phosphates at this temperature, resulting in separation of REEs and other elements. After that, recovery of phosphoric acid and production of gypsum are achieved by adopting concentrated sulfuric acid at ambient temperature and the phosphoric acid can be recycled to decompose crude phosphate rock [3,25].

3.6 Analysis of leaching residue for different leaching time

In order to study the leaching process, chemical analysis of leaching residue after different leaching time was conducted and the results are presented in Table 4. The content of P_2O_5, CaO, and MgO declined gradually, indicating that fluorapatite, calcite, and dolomite were dissolving with the prolonging of time. The content of F decreased at the first stage and increased slightly at the second stage. At the first stage, dissolving of fluorapatite was the main factor, thus the content of F decreased. At the second stage, the content of F was mainly governed by the formation of F-related precipitation, leading to slight increase of F in the leaching residue. The content of SiO_2, Fe_2O_3, Al_2O_3, and SO_3 increased gradually, indicating that the minerals containing Si, Fe, Al, and S were not as soluble as those of fluorapatite, calcite, and dolomite in phosphoric acid solution.

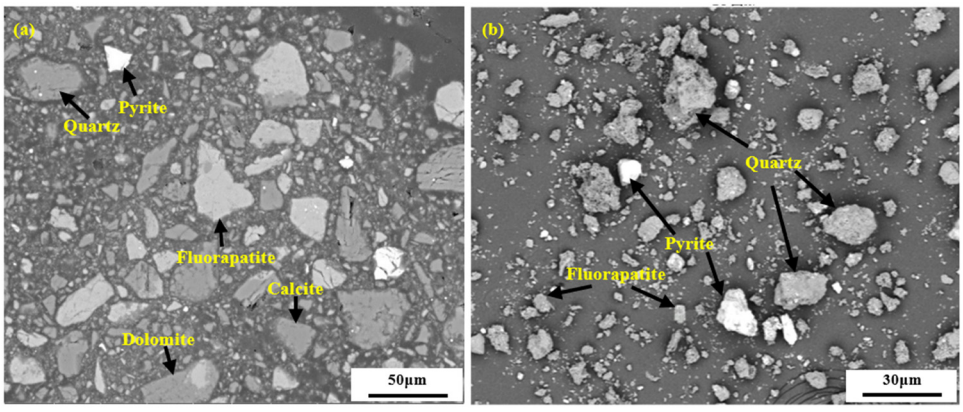

Figure 9: SEM images of phosphate ore before (a) and after (b) leaching for 120 min.

Leaching efficiencies of various elements at different leaching time were calculated/detected and the results were plotted in Figure 8. The leaching efficiencies increased sharply at the first half an hour and changed mildly with the prolonging of time. The leaching efficiencies almost increased following the order: Si, Al, S, Fe, F, REE, P, Ca, Mg.

Figure 9 presents SEM images of the leaching residue before and after leaching for 120 min. The fluorapatite particle size markedly reduced; pyrite and quartz particle size moderately decreased, while dolomite and calcite particles were not detected after leaching for 120 min. In addition, the peak intensity of dolomite, fluorapatite, and calcite decreased with the prolonging of leaching time (Figure 10), suggesting the dissolving of these minerals. The peak intensity of quartz, pyrite, and muscovite increased with the increase of leaching time, indicating that these minerals were not as soluble as dolomite, fluorapatite, and calcite (Figure 10). What is more, calcite dissolves faster than dolomite [26,27]. Combining these results with Figure 8 and Table 3, it might be concluded that leaching difficulties of minerals decreased following the order: quartz, aluminosilicate, pyrite, fluorapatite, dolomite, and calcite.

The leaching efficiencies of P and F were virtually identical after leaching for 30 min; thereafter, leaching efficiency of F was lower than that of P. In addition, the leaching efficiency of Si declined after 30 min; it might be concluded that insoluble fluorosilicate was formed after 30 min of leaching time. However, the content of fluorosilicate might be too low to be detected by XRD. The leaching efficiencies of Fe and S were almost the same, indicating that part of pyrite was dissolved in the acid hydrolysis solution. The leaching efficiency of Al was higher than that of Si, which could be attributed to two reasons. First, the solubility of quarts was lower than that of aluminosilicate. Secondly, aluminum oxide octahedron was not as stable as silicon oxide tetrahedron, thus Al was easier to be dissolved from aluminosilicate than Si [28].

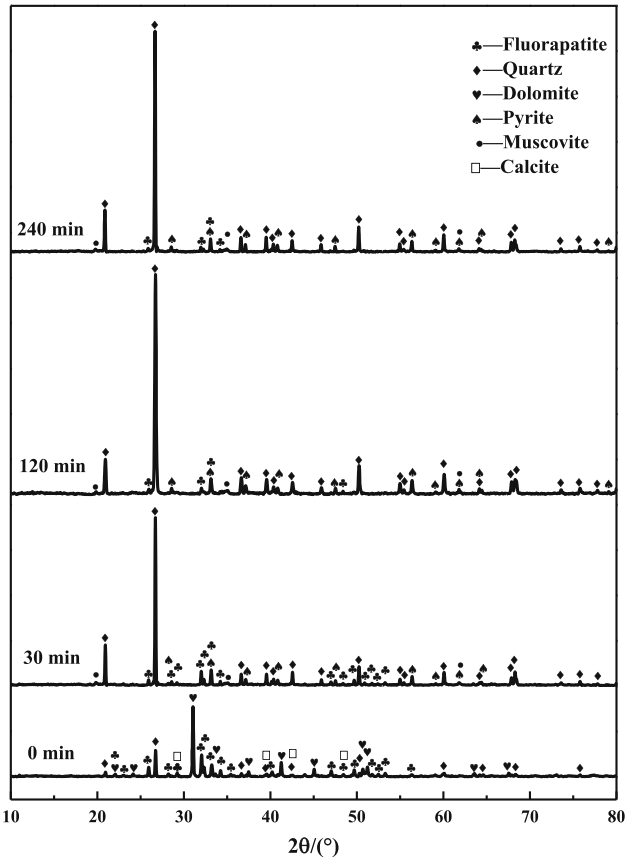

Figure 10: XRD spectrum of phosphate ore after leaching for different time.

4 Conclusion

REEs were mainly present in fluorapatite and dolomite in Zhijin phosphate ore. The optimum leaching conditions for Zhijin phosphate ore using phosphoric acid were as follows: phosphoric acid concentration in the initial leaching pulp of 25–35%, temperature of 60°C, ratio of liquid to solid of 12–14 mL/g, agitation speed of 220 rpm, and leaching time of more than 120 min. The REEs and phosphorus in the Zhijin phosphate ore could be leached out efficiently, reaching efficiencies of 97.8% and 99.7%, respectively. REE leaching efficiency showed similar trends to those of phosphorus.

In Zhijin phosphate ore, leaching efficiencies of minerals by phosphoric acid increased following the order: quartz, aluminosilicate, pyrite, fluorapatite, dolomite, and calcite. The most part of dissoluble REEs, phosphorous, and other dissolvable elements were decomposed in the first half an hour. Insoluble fluorosilicate might be formed during the leaching of Zhijin phosphate ore by phosphoric acid.

Funding information: This research was funded by Hubei Tailings (Slag) Resource Utilization Engineering Technology Research Center Project, grant number No. 2019ZYYD070, China Geological Survey Project, grant number No. DD20190626, Scientific Research Foundation of Wuhan Institute of Technology (K202064), and Open Foundation of State Environmental Protection Key Laboratory of Mineral Metallurgical Resources Utilization and Pollution Control (HB201912).

Author contributions: Conceptualization: D. H. and Z. L.; data curation: Z. L., H. Z., and H. L.; formal analysis: J. D. and H. Z.; funding acquisition: D. H.; investigation: Z. X.; methodology: Z. L. and Z. X.; project administration: D. H.; resources: D. H.; supervision: D. H.; validation: J. D. and D. H.; visualization: Z. L. and H. L.; writing – original draft: Z. X.; writing – review and editing: Z. L. All authors have read and agreed to the published version of the manuscript.

Conflict of interest: Authors state no conflict of interest.

References

[1] Zhang L, Xie F, Li S, Yin S, Peng J, Ju S. Solvent extraction of Nd (III) in a Y type microchannel with 2-ethylhexyl phosphoric acid-2-ethylhexyl ester. Green Process Synth. 2015;4(1):3–10. doi: 10.1515/gps-2014-0095.

[2] Lin G, Zhang L, Yin S, Peng J, Li S, Xie F. Study on the calcination experiments of rare earth carbonates using microwave heating. Green Process Synth. 2015;4(4):329–36. doi: 10.1515/gps-2015-0040.

[3] Wu S, Zhao L, Wang L, Huang X, Zhang Y, Feng Z, et al. Precipitation-dissolution behaviors of rare earth ions in H_3PO_4-$Ca(H_2PO_4)_2$ solutions. J Rare Earth. 2019;37(5):520–7. doi: 10.1016/j.jre.2018.06.013.

[4] Emsbo P, McLaughlin PI, Breit GN, du Bray EA, Koenig AE. Rare earth elements in sedimentary phosphate deposits: solution to the global REE crisis? Gondwana Res. 2015;27(2):776–85. doi: 10.1016/j.gr.2014.10.008.

[5] Wu S, Wang L, Zhao L, Zhang P, El-Shall H, Moudgil B, et al. Recovery of rare earth elements from phosphate rock by hydrometallurgical processes–a critical review. Chem Eng J. 2018;335:774–800. doi: 10.1016/j.cej.2017.10.143.

[6] Liang H, Zhang P, Jin Z, DePaoli DW. Rare earth and phosphorus leaching from a flotation tailings of florida phosphate rock. Minerals. 2018;8(9):416. doi: 10.3390/min8090416.

[7] McArthur JM, Walsh JN. Rare-earth geochemistry of phosphorites. Chem Geol. 1984;47(3–4):191–220. doi: 10.1016/0009-2541(84)90126-8.

[8] Al-Thyabat S, Zhang P. Extraction of rare earth elements from upgraded phosphate flotation tailings. Min Metall Proc. 2016;33(1):23–30. doi: 10.19150/mmp.6464.

[9] Banihashemi SR, Taheri B, Razavian SM, Soltani F. Selective nitric acid leaching of rare-earth elements from calcium and phosphate in fluorapatite concentrate. J Mater. 2019;71(12):4578–87. doi: 10.1007/s11837-019-03605-6.

[10] Bandara AMTS, Senanayake G. Dissolution of calcium, phosphate, fluoride and rare earth elements (REEs) from a disc of natural fluorapatite mineral (FAP) in perchloric, hydrochloric, nitric, sulphuric and phosphoric acid solutions: a kinetic model and comparative batch leaching of major and minor elements from FAP and RE-FAP concentrate. Hydrometallurgy. 2019;184:218–36. doi: 10.1016/j.hydromet.2018.09.002.

[11] Abd El-Mottaleb M, Cheira MF, Gouda GA, Ahmed AS. Leaching of rare earth elements from Egyptian Western desert phosphate rocks using HCl. Chem Adv Mater. 2016;1(1):33–40.

[12] Liang H, Zhang P, Jin Z, DePaoli D. Rare-earth leaching from Florida phosphate rock in wet-process phosphoric acid production. Min Metall Proc. 2017;34(3):146–53. doi: 10.19150/mmp.7615.

[13] Soltani F, Abdollahy M, Petersen J, Ram R, Becker M, Koleini SJ, et al. Leaching and recovery of phosphate and rare earth elements from an iron-rich fluorapatite concentrate: Part I: direct baking of the concentrate. Hydrometallurgy. 2018;177:66–78. doi: 10.1016/j.hydromet.2018.02.014.

[14] Brahim FB, Mgaidi A, Elmaaoui M. Kinetics of leaching of Tunisian phosphate ore particles in dilute phosphoric acid solutions. Can J Chem Eng. 1999;77(1):136–42. doi: 10.1002/cjce.5450770123.

[15] Wu S, Zhao L, Wang L, Huang X, Zhang Y, Feng Z, et al. Simultaneous recovery of rare earth elements and phosphorus from phosphate rock by phosphoric acid leaching and selective precipitation: towards green process. J Rare Earth. 2019;37(6):652–8. doi: 10.1016/j.jre.2018.09.012.

[16] Soltani F, Abdollahy M, Petersen J, Ram R, Koleini SJ, Moradkhani D. Leaching and recovery of phosphate and rare earth elements from an iron-rich fluorapatite concentrate: Part II: selective leaching of calcium and phosphate and acid baking of the residue. Hydrometallurgy. 2019;184:29–38. doi: 10.1016/j.hydromet.2018.12.024.

[17] Bakry AR, Hashim MD, Elwy AM. Thermodynamic and kinetic studies of uranium and rees leaching by oxalic acid from Abu-Tartur phosphate rock, Western Desert, Egypt. Radiochemistry. 2020;62(3):359–67. doi: 10.1134/S106636222003008X.

[18] Ashraf M, Zafar ZI, Ansari TM. Selective leaching kinetics and upgrading of low-grade calcareous phosphate rock in succinic acid. Hydrometallurgy. 2005;80(4):286–92. doi: 10.1016/j.hydromet.2005.09.001.

[19] Wang L, Long Z, Huang X, Yu Y, Cui D, Zhang G. Recovery of rare earths from wet-process phosphoric acid. Hydrometallurgy. 2010;101(1–2):41–47. doi: 10.1016/j. hydromet. 2009.11.017.

[20] Reddy BR, Kumar BN, Radhika S. Soli-liquid extraction of terbium from phosphoric acid medium using bifunctional phosphinic acid resin, Tulsion CH-96. Solvent Extr Ion Exc. 2009;27(5–6):695–711. doi: 10.1080/07366290903270031.

[21] Cetiner ZS, Wood SA, Gammons CH. The aqueous geochemistry of the rare earth elements. Part XIV. The solubility of rare earth element phosphates from 23 to 150°C. Chem Geol. 2005;217(1–2):147–69. doi: 10.1016/j.chemgeo.2005.01.001.

[22] Altschuler ZS, Berman S, Cuttitta F. Rare earths in phosphorites–geochemistry and potential recovery. U.S. Geological Survey Professional Papers. 1967;525B:1–9.

[23] Battsengel A, Batnasan A, Narankhuu A, Haga K, Watanabe Y, Shibayama A. Recovery of light and heavy rare earth elements from apatite ore using sulphuric acid leaching, solvent extraction and precipitation. Hydrometallurgy. 2018;179:100–9. doi: 10.1016/j.hydromet. 2018.05.024.

[24] Gergoric M, Ravaux C, Steenari BM, Espegren F, Retegan T. Leaching and recovery of rare-earth elements from neodymium magnet waste using organic acids. Metals. 2018;8(9):721. doi: 10.3390/met8090721.
[25] Li Z, Xie Z, Deng J, He D, Zhao H, Liang H. Leaching kinetics of rare earth elements in phosphoric acid from phosphate rock. Metals. 2021;11:239. doi: 10.3390/met11020239.
[26] Guo H, Wang YB, Ni XM, Tao CQ, Han WL. Chemical kinetics of Ca/Mg elements from calcite/dolomite in carbonic acid solution. China Coal Soc. 2016;41:1806–12. (in Chinese).
[27] Huang S, Hou Z. Spatio-temporal variation of subsurface porosity and permeability and its influential factors. Acta Sedimentol Sin. 2001;19(2):224–32.
[28] Grim RE. Clay mineralogy. LWW. 1953;76(4):317.